Ecography

ECOG-02513
Cramer, K. L., O'Dea, A., Carpenter, C. and Norris, R. D. 2017. TA 3000 year record of Caribbean reef urchin communities reveals causes and consequences of long-term decline in *Diadema antillarum*. – Ecography doi: 10.1111/ecog.02513

Supplementary material

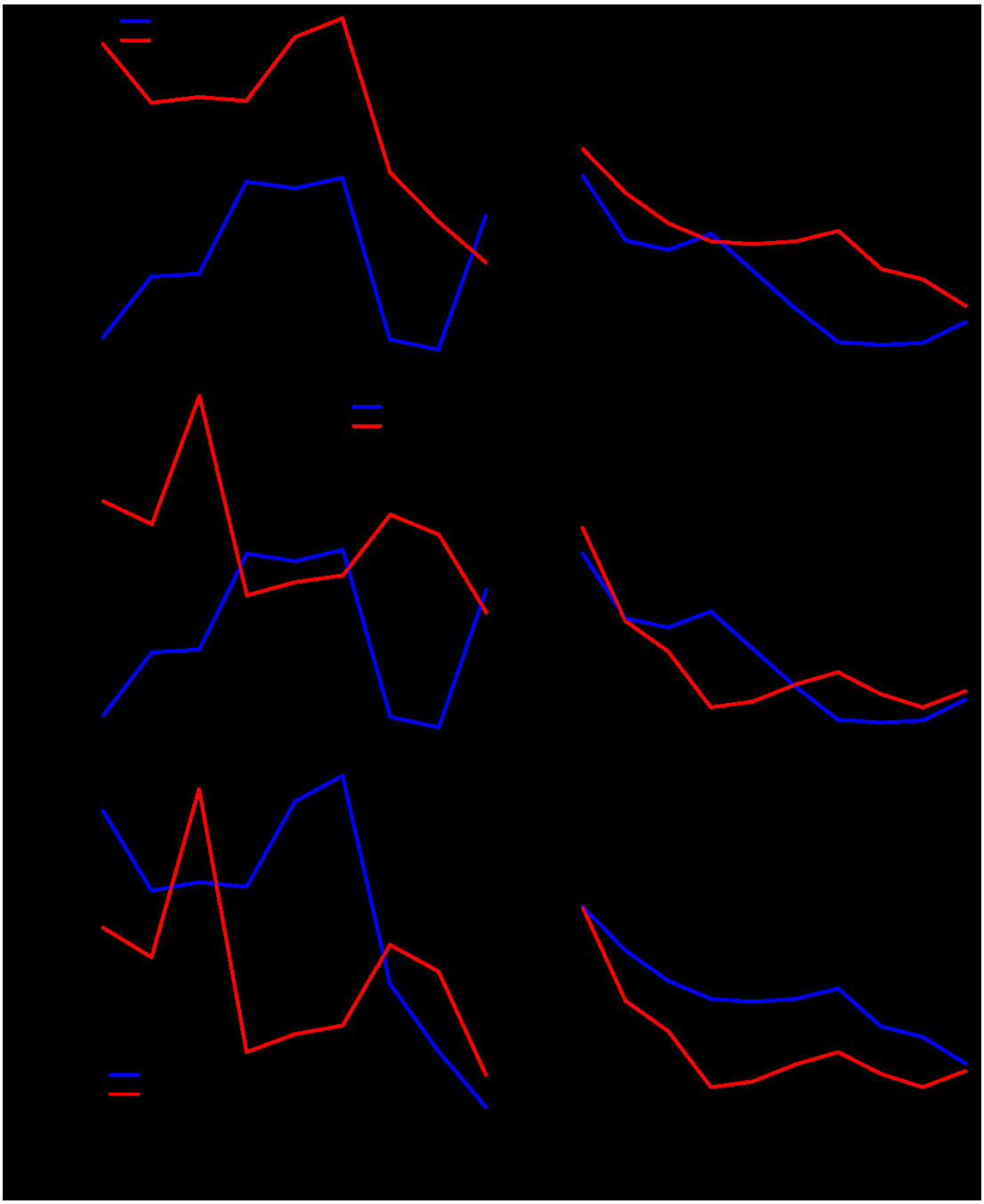

Figure A2. Diagnostic plots for multispatial convergent cross mapping (CCM) results shown in Figure 3. For each variable pairing, (a) embedding dimension value that corresponded to highest Pearson correlation coefficient (rho) was selected for analysis, and (b) rho was sufficiently high at a short number of prediction steps and declined with increasing prediction time, confirming assumptions of nonlinearity and nonrandomness.

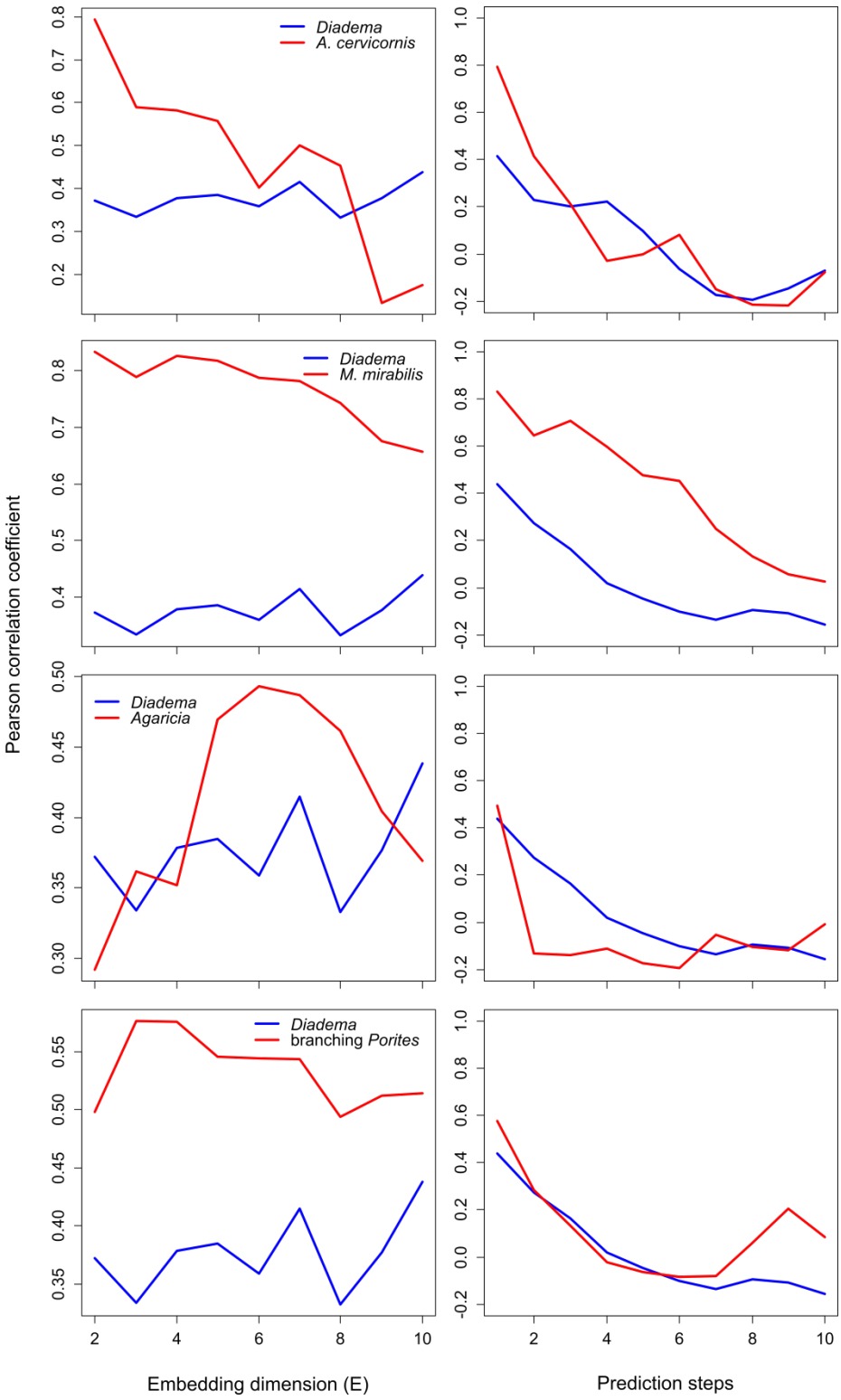

Figure A3. Diagnostic plots for multispatial convergent cross mapping (CCM) results shown in Figure 4. For each variable pairing, (a) embedding dimension value that corresponded to highest Pearson correlation coefficient (rho) was selected for analysis, and (b) rho was sufficiently high at a short number

of prediction steps and declined with increasing prediction time, confirming assumptions of nonlinearity and nonrandomness.

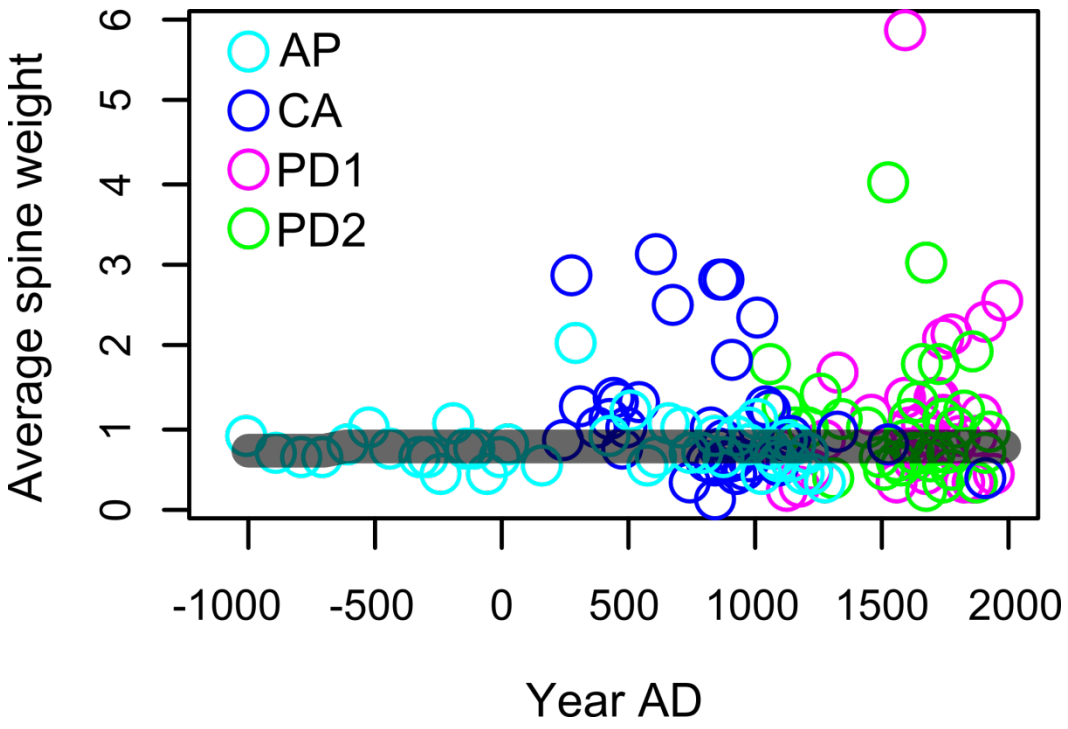

Figure A4. Average individual weight (in mg) of *Diadema* spine fragments (total weight / total abundance). Line is loess smooth for samples from all cores combined. AP = Airport Point, CA = Cayo Adriana, PD1 = Punta Donato core 1, PD2 = Punta Donato core 2.

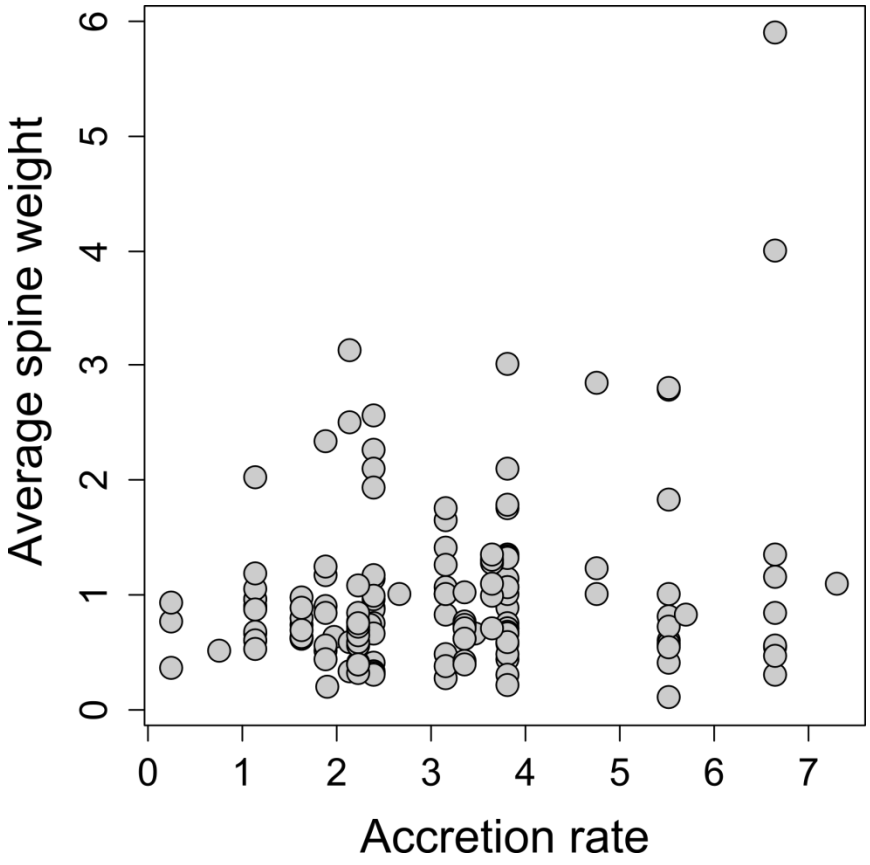

Figure A5. Average individual weight (in mg) of *Diadema* spine fragments and accretion rate (mm/year).

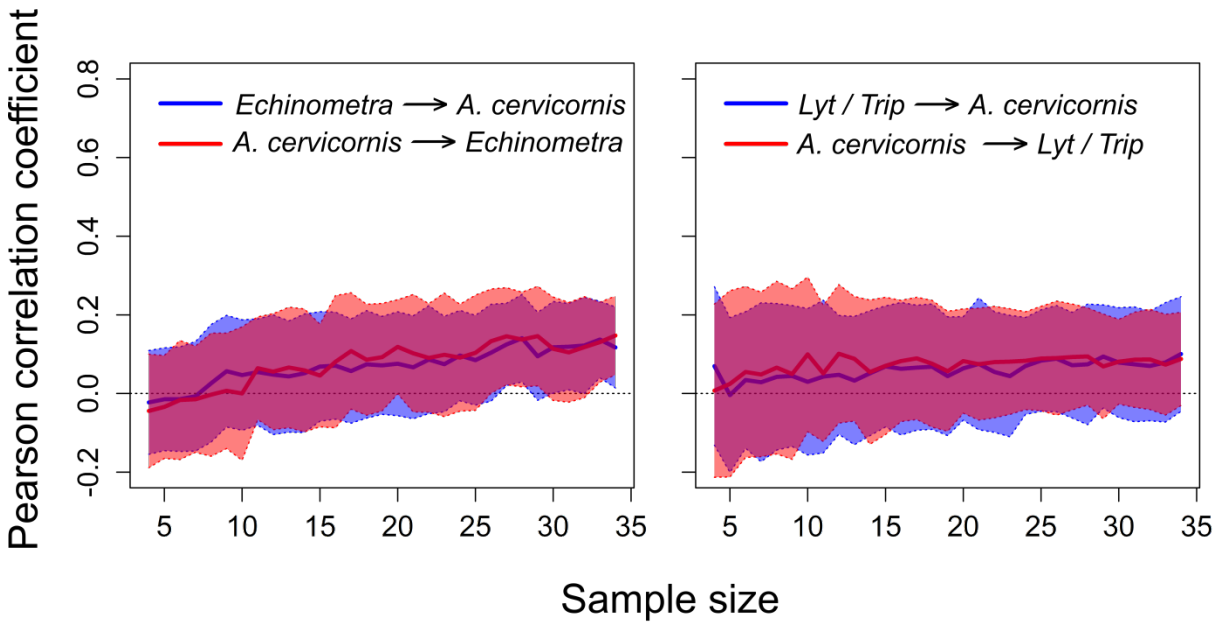

Figure A6. Multispatial convergent cross mapping (CCM) results showing absence of causal relationships between relative abundance of staghorn coral *A. cervicornis* and abundance of *Echinometra* and *Lytechinus / Tripneustes* urchins (spine weight / dry weight of 0.5-2 mm sediment fraction). Lines and shaded regions show mean ± SD from 100 bootstrapped iterations. Causal forcing is indicated when the Pearson correlation coefficient is significantly greater than zero for larger sample sizes (number of core samples, including all spatial replicates in the composite time series) and when correlation coefficient increases significantly with increasing number of core samples. *A. cervicornis* abundant in Cayo Adriana core only, therefore this analysis only includes samples from this core.

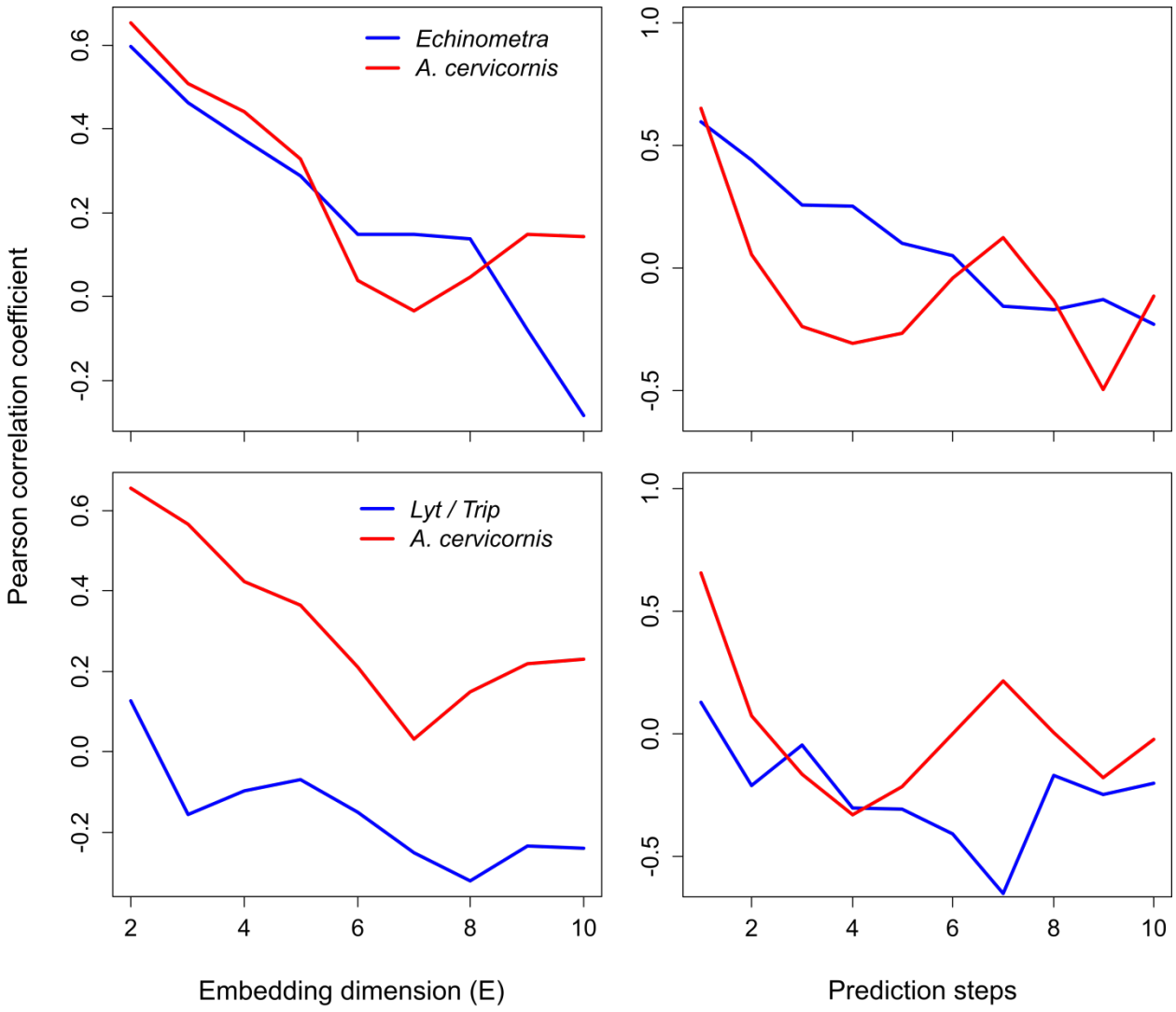

Figure A7. Diagnostic plots for multispatial convergent cross mapping (CCM) results shown in Figure A5. For each variable pairing, (a) embedding dimension value that corresponded to highest Pearson correlation coefficient (rho) was selected for analysis, and (b) rho was sufficiently high at a short number of prediction steps and declined with increasing prediction time, confirming assumptions of nonlinearity and nonrandomness.

Table A1. MC-ICP-MS ^{230}Th ages of coral fragments obtained from reef matrix cores collected in the Caribbean. Two cores were obtained per site: one core was "well-dated" while the second "replicate" core was constrained by only two dates.

Core	Core position (mm from top)	Sample weight (g)	U (ppm)	^{232}Th (ppb)	(^{230}Th/^{232}Th)	(^{230}Th/^{238}U)	[a]δ^{234}U	Time of chemistry (AD)	Uncorr. ^{230}Th age (BC/AD)	[b]Corr. ^{230}Th age (BC/AD)	[c]Corr. ^{230}Th age (BP)
Airport Point	0	0.15459	2.9751 ± 0.0015	2.357 ± 0.056	30.26 ± 0.74	0.007902 ± 0.000048	146.0 ± 1.3	2014.83	1260.4 ± 4.7	1280 ± 6	669.7 ± 6.2
	225	0.15552	3.0049 ± 0.0012	0.794 ± 0.027	88.8 ± 3.1	0.007728 ± 0.000072	147.0 ± 1.2	2014.83	1277.8 ± 6.9	1287 ± 7	662.5 ± 7.2
	425	0.15160	2.8445 ± 0.0012	2.93 ± 0.31	32.7 ± 3.4	0.011069 ± 0.000049	147.2 ± 1.0	2014.83	957.8 ± 4.8	982 ± 7	967.6 ± 7.3
	675	0.15133	2.8099 ± 0.0013	0.654 ± 0.025	142.6 ± 5.5	0.010941 ± 0.000055	145.2 ± 1.1	2014.83	968.3 ± 5.4	978 ± 6	972.3 ± 5.8
	1755	0.15369	2.7791 ± 0.0013	2.18 ± 0.11	80.4 ± 4.0	0.02077 ± 0.00010	147.7 ± 1.4	2014.83	24 ± 10	44 ± 11	1906 ± 11
	2960	0.17689	2.8705 ± 0.0012	4.04 ± 0.25	52.9 ± 3.3	0.024566 ± 0.000083	146.5 ± 1.3	2014.83	-345.9 ± 8.5	-314 ± 11	2264 ± 11
	4085	0.16048	2.9114 ± 0.0013	0.788 ± 0.039	352 ± 18	0.03135 ± 0.00013	146.4 ± 1.1	2014.83	-1007 ± 13	-997 ± 13	2947 ± 13
Airport Point (replicate)	0	0.19340	2.7590 ± 0.0014	2.075 ± 0.066	43.76 ± 1.41	0.010846 ± 0.000067	149.6 ± 1.0	2014.83	981.4 ± 6.4	1001 ± 8	949.2 ± 7.5
	3200	0.15195	2.9495 ± 0.0015	4.11 ± 0.14	65.44 ± 2.25	0.03002 ± 0.00011	146.3 ± 0.9	2014.83	-877 ± 11	-846 ± 12	2796 ± 12
Cayo Adriana	0	0.30314	2.6480 ± 0.0010	1.7964 ± 0.0022	4.995 ± 0.075	0.001117 ± 0.000017	148.4 ± 0.9	2013.89	1907.7 ± 1.6	1925.9 ± 4.0	24.1 ± 4.0
	200	0.15626	3.08156 ± 0.00090	0.10792 ± 0.00059	788.46 ± 7.32	0.009100 ± 0.000068	147.4 ± 0.7	2014.83	1146.7 ± 6.5	1152 ± 7	798.1 ± 6.6
	400	0.16861	2.6144 ± 0.0011	2.6300 ± 0.0033	37.50 ± 0.19	0.012432 ± 0.000062	147.5 ± 0.9	2014.83	827.2 ± 6.0	852 ± 8	1098.2 ± 7.8
	600	0.28834	2.56942 ± 0.00064	1.1296 ± 0.0011	78.38 ± 0.35	0.011357 ± 0.000050	147.1 ± 0.6	2013.89	927.6 ± 4.9	941.5 ± 5.6	1008.5 ± 5.6
	1225	0.12145	2.9608 ± 0.0024	0.40842 ± 0.00054	273.83 ± 2.54	0.01245 ± 0.00011	146.5 ± 1.2	2013.89	822 ± 11	829.4 ± 11.2	1121 ± 11
	1825	0.23607	2.73034 ± 0.00071	0.9260 ± 0.0011	137.71 ± 0.55	0.015392 ± 0.000059	146.9 ± 0.6	2013.89	538.9 ± 5.7	550.5 ± 6.2	1399.5 ± 6.2
	2410	0.22407	2.57093 ± 0.00069	4.9181 ± 0.0037	27.54 ± 0.12	0.017364 ± 0.000074	146.8 ± 0.6	2013.89	348.3 ± 7.2	390.4 ± 11.1	1560 ± 11
	3010	0.15027	2.6653 ± 0.0012	2.4439 ± 0.0030	61.18 ± 0.31	0.018489 ± 0.000092	147.6 ± 1.2	2013.88	240.8 ± 9.1	263.6 ± 10.2	1686 ± 10
Cayo Adriana (replicate)	0	0.15520	3.4257 ± 0.0016	1.2440 ± 0.0027	76.92 ± 0.44	0.009205 ± 0.000049	145.6 ± 1.3	2014.83	1135.2 ± 4.8	1146 ± 5	803.7 ± 5.3
	4855	0.18861	3.5112 ± 0.0023	2.5673 ± 0.0032	140.59 ± 0.60	0.03388 ± 0.00014	145.4 ± 1.1	2014.83	-1257 ± 14	-1239 ± 15	3189 ± 15
Punta Donato1	0	0.23014	2.58328 ± 0.00083	0.9665 ± 0.0013	3.610 ± 0.089	0.000445 ± 0.000011	146.8 ± 1.0	2013.89	1971.5 ± 1.0	1984.1 ± 2.8	-34.1 ± 2.8
	535	0.18008	2.8251 ± 0.0015	1.647 ± 0.062	14.77 ± 0.57	0.002838 ± 0.000023	146.7 ± 1.1	2014.83	1744.6 ± 2.2	1761 ± 4	189.3 ± 4.0
	1135	0.12697	2.94011 ± 0.00087	0.86495 ± 0.00090	45.45 ± 0.46	0.004406 ± 0.000045	147.8 ± 0.8	2013.89	1593.9 ± 4.3	1604.3 ± 4.8	345.7 ± 4.8
	2185	0.19065	2.55917 ± 0.00058	0.69644 ± 0.00092	67.56 ± 0.55	0.006059 ± 0.000049	147.2 ± 0.6	2013.89	1435.7 ± 4.7	1446.4 ± 5.2	503.6 ± 5.2
	3140	0.16530	2.77901 ± 0.00079	0.90693 ± 0.00093	85.65 ± 0.67	0.009212 ± 0.000071	147.5 ± 0.8	2013.89	1133.9 ± 6.9	1145.2 ± 7.2	804.8 ± 7.2
	3235	0.15000	2.9921 ± 0.0016	3.1078 ± 0.0060	28.65 ± 0.19	0.009806 ± 0.000063	146.6 ± 1.1	2013.88	1076.1 ± 6.1	1100.7 ± 7.9	849.3 ± 7.9
Punta Donato2	0	0.16196	2.7810 ± 0.0016	1.6070 ± 0.0014	4.125 ± 0.069	0.000786 ± 0.000013	148.3 ± 1.0	2014.83	1940.2 ± 1.3	1956 ± 3	-6.3 ± 3.5
	3245	0.15443	2.7268 ± 0.0015	2.8458 ± 0.0029	34.74 ± 0.22	0.011949 ± 0.000076	146.4 ± 1.0	2014.83	872.5 ± 7.4	898 ± 9	1052.4 ± 8.9

Ratios in parentheses are activity ratios calculated from atomic ratios using decay constants of Cheng et al. (2000). All values have been corrected for laboratory procedural blanks. All errors reported as 2-sigma (2σ). Uncorrected ^{230}Th ages (BC/AD) were calculated using Isoplot/EX 3.0 program (Ludwig, 2003), where BC = Before Christ and AD = Anno Domini.

[a]$\delta^{234}U = [(^{234}U/^{238}U)-1] \times 1000$.

[b]^{230}Th ages were corrected using a modelled two-component correction value based on the equation in Clark et al. (2014) where the $^{232}Th_{dead}$ value used was the measured ^{232}Th value (ppb) in the non-living coral sample of this study. $^{232}Th_{live}$ was assumed to approximate the mean measured ^{232}Th value (ppb) of living coral specimens (0.95 ppb) found on the GBR (Great Barrier Reef) as no local values have been obtained for the Caribbean. Similarly, the $^{230}Th/^{232}Th_{live}$ value represents or approximates the isotopic composition of the hydrogenous component in the dead coral skeleton with an activity value of 1.08 ± 20% determined from live corals of the GBR. $^{230}Th/^{232}Th_{sed}$ is the detrital component represented by a by a mean activity value of 0.61 ± 20% from isochron derived initial $^{230}Th/^{232}Th$ values obtained from dead *Porites* coral skeletons of the GBR.

[c]Corrected ^{230}Th age in years before present (BP; where 'present' is 1950 AD).

References:

Cheng, H., et al. 2000. The half-lives of uranium-234 and thorium-230. - *Chem. Geol.* 169: 17e33.

Clark, T.R., et al. 2014. Testing the precision and accuracy of the U-Th chronometer for dating coral mortality events in the last 100 years. - *Quat. Geochronol.* 23: 35-45.

Ludwig, K.R., 2003. Users' Manual for Isoplot/Ex Version 3.0: a Geochronological Toolkit for Microsoft Excel. - Berkeley Geochronology Centre, Berkeley. Special Publication No.3.